

The PADME experiment at LNF-INFN

Venelin Kozhuharov^a for the PADME collaboration *

^a*Faculty of Physics, Sofia University “St. Kl. Ohridski”,
5 J. Bourchier Blvd., 1164 Sofia, Bulgaria*

E-mail: venelin@phys.uni-sofia.bg

Despite the impressive success of the Standard Model (SM) in describing nature, it still fails in finding the answers for a few astrophysics phenomena, including the lack of antimatter in the Universe and what Dark Matter is made of. Recently, models proposing the existence of a whole new world of particles, the so-called Dark sector (DS), regained interest. The PADME experiment at LNF-INFN aims to search for new light states, which may act as a portal between the SM and the DS, employing positron-on-target annihilation technique. Operating since autumn 2018, PADME accomplished successfully its first two periods of data taking at the DAΦNE Linac, corresponding to $O(10^{13})$ positrons on target. The sensitivity to new light states depends on the reliable reconstruction of the events in a high instantaneous rate environment, precise knowledge of the background processes, and detailed Monte Carlo simulation of the experimental setup. The design and the construction of the PADME experiment is described and the first physics results using part of the collected data are presented.

*11th International Conference of the Balkan Physical Union (BPU11),
28 August - 1 September 2022
Belgrade, Serbia*

*The PADME collaboration: A. P. Caricato, M. Martino, I. Oceano, F. Oliva, S. Spagnolo (INFN Lecce and Salento Univ.), G. Chiodini (INFN Lecce), F. Bossi, R. De Sangro, C. Di Giulio, D. Domenici, G. Finocchiaro, L. G. Foggetta, M. Garattini, A. Ghigo, P. Gianotti, I. Sarra, T. Spadaro, E. Spiriti, C. Taruggi, E. Vilucchi (INFN Laboratori Nazionali di Frascati), V. Kozhuharov (Faculty of Physics, Sofia Univ. “St. Kl. Ohridski” and INFN Laboratori Nazionali di Frascati), S. Ivanov, Sv. Ivanov, R. Simeonov (Faculty of Physics, Sofia Univ. “St. Kl. Ohridski”), G. Georgiev (Sofia Univ. “St. Kl. Ohridski” and INRNE Bulgarian Academy of Science), Ferrarotto, E. Leonardi, P. Valente, A. Variola (INFN Roma1), E. Long, G. C. Organtini, G. Piperno, M. Raggi (INFN Roma1 and “Sapienza” Univ. Roma), S. Fiore (ENEA Frascati and INFN Roma1), V. Capirossi, F. Iazzi, F. Pinna (Politecnico of Torino and INFN Torino), A. Frankenthal (Princeton University).

1. Introduction

Among the enormous variety of particle physics experimental results in last two decades, almost all consistent with the Standard Model (SM) predictions, few smoking guns ask for a more detailed attention. The anomalous magnetic moment of the muon $a_\mu = (g_\mu - 2)/2$ is a long-lasting experimental quest. The discrepancy between the new experimental results [1] and the expected value within the Standard Model

$$\Delta a_\mu = (251 \pm 59) \times 10^{-11} \quad (1)$$

is more than four standard deviations. This points towards the existence of new contribution non accounted in the present calculations.

Another striking signature influencing our understanding of the particle content comes from nuclear physics measurements of light even-even nuclei. After the initial observation of a substructure in the angular distribution and thus the invariant mass distribution of the internally created e^+e^- pair in the de-excitation of a ^8Be state [2], pointing towards the mediation of the process through a new particle X with mass $m_X \simeq 17$ MeV, similar substructures were also detected in other light nuclei. The announced results by the study of ^{12}C [3] and ^4He [4] are consistent in mass with the $X17$ hypothesis and present a major challenge to the particle physics and experimental community.

Both, the a_μ discrepancy and the $X17$ hypothesis can be resolved by the possible existence of new particles with mass in the MeV range. In fact, models proposing new light vector fields have been studied already in the 80s [5]. Usually a new degree of freedom with similar characteristics to the ordinary photon is introduced, the so-called dark photon [6]. The dark photon interacts with the SM fermions either through kinetic mixing with the ordinary photon or through non-vanishing, albeit very small, charges q_f which the SM particles possess with respect to a newly introduced $U(1)$ gauge symmetry

$$\mathcal{L} \sim g' q_f \bar{\psi}_f \gamma^\mu \psi_f A'_\mu, \quad (2)$$

where g' is the universal coupling constant of the new interaction. The parameter space of this new state is given by its mass, $m_{A'}$ or m_X and its coupling $g = g' \times q_f$. In the most general case this new degree of freedom could be scalar, pseudo-scalar or vector [7] and the interaction can be either through vector or through (pseudo-)tensor currents [8].

By requiring this new light particle to be a portal to a whole hidden sector of neutral with respect to SM gauge groups particles, an explanation of the Dark Matter content of the Universe can naturally be incorporated.

The high predictive power of the aforementioned models led to their recent revival and several experimental setups were constructed and operated to address the possible existence of such new light states.

2. PADME experimental setup

The PADME experiment [9] at Laboratori Nazionali di Frascati, INFN uses a positron beam directed to a thin active target to probe the production of new light particles in the positron-on-target annihilation process.

PADME exploits the positron beam from the DAΦNE accelerator complex, occupying the former hall¹ of the Beam Test Facility at LNF-INFN. The Linac provides 50 bunches per second with either electrons or positrons, each with duration of up to about 250 ns [11, 12]. Each second one bunch is used for monitoring purposes while the other 49 are utilized by the PADME apparatus. A schematic of the PADME detector setup is shown in Fig. 1.

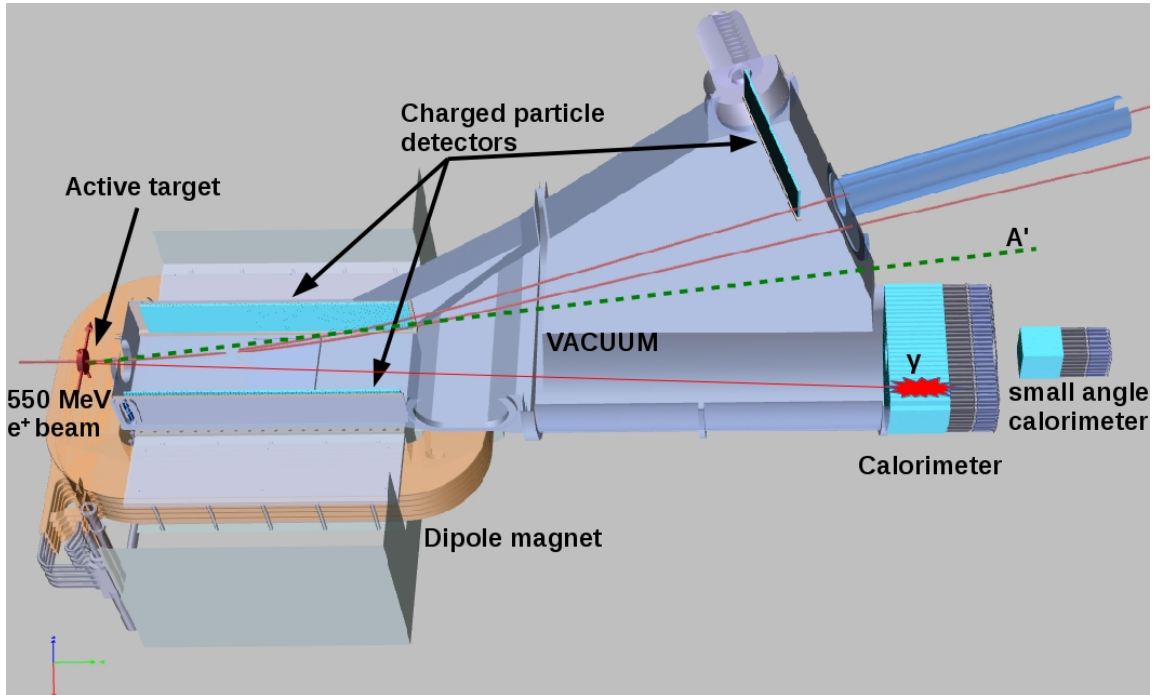


Figure 1: Schematics of the PADME experiment during RUNI and RUNII.

The major components of the experiment are:

- Active target [14]: The positron beam from the DAΦNE Linac interacts in a 100 μm thick diamond target with transverse dimensions of $2 \times 2 \text{ cm}^2$. Two orthogonal sets of 1 mm wide graphite strips, realized by excimer laser on the two sides of the target, detect the ionization induced by the passage of the beam particles and allow the reconstruction of the beam position (both x and y coordinates) and the particle multiplicity bunch by bunch.
- Electromagnetic calorimeter (ECal) [13]: A high granularity inorganic crystal calorimeter, placed 3.4 m downstream of the diamond target, measures the energy and impact point of the impinging photons and electrons. A total of 616 bismuth germanate (BGO) crystals with dimensions $21 \times 21 \times 230 \text{ mm}^3$ are arranged in a $\approx 60 \text{ cm}$ diameter ring with inner hole with size of $105 \times 105 \text{ mm}^2$. The light is registered by HZC XP1911 photomultiplier tubes.
- Small angle calorimeter (SAC) [15]: A fast Cherenkov detector registers the particles passing through the ECal inner hole. It is constructed as 5×5 segmented matrix of PbF_2 crystals. Together with the ECal the SAC serves as multiphoton event detector and improves significantly the background rejection.

¹new hall with a dedicated beam line has been put in operation after the start of PADME

- Charged particle detectors (Vetos) [16, 17]: Three sets of arrays of plastic scintillator bars, the PVeto, the EVeto, and the HEPVeto are used to detect the charged particles, which are deflected by the ≈ 0.5 T dipole magnetic field. The scintillating light is captured by a WLS fiber placed inside a groove along the square cross-section bars and is transmitted to a custom designed readout system based on Silicon photomultipliers. The charged particle detector system is located inside the PADME vacuum vessel and the PVeto and the EVeto are operated inside the magnetic field.
- Silicon pixel detectors (TimePix and MIMOSA): Two different silicon pixel detector technologies are used in PADME. The MIMOSA, a monolith active pixel sensor, is aimed at beam parameters measurement during the beam tuning. In addition, downstream of the vacuum chamber, an array of 6×2 TimePix sensors, each with 256×256 pixels, is placed. The TimePix allows precise monitoring of the beam multiplicity, divergence, and spread bunch by bunch.
- Data acquisition system (DAQ): The majority of the DAQ system is built around the CAEN V1742 digitizer board, which is operated at different sampling frequency depending on the detector - 1 GS/s for the ECal and 2.5 GS/s for the Vetos and SAC. A custom developed trigger module receives signals from the Linac infrastructure, from ECal calibration system, or random events and produces a common trigger distributed to the digitization modules. The data are collected in a board streaming mode by a custom developed DAQ software and are merged in event oriented mode by follow-up processing chain. The output data are stored in ROOT trees for subsequent analysis.

A detailed assessment of the performance of the PADME subdetectors can be found in [18]. The physics results extraction is made possible by a detailed GEANT4 based Monte Carlo simulation of the setup. The simulation package also includes propagation of the beam particles through the beam optic components, to precisely account for the beam induced background [19].

3. Measurements with PADME RUN-I and RUN-II

PADME started taking data in the autumn, 2018. The first data taking period, RUN-I, lasted about three months till the end of February, 2019, leading to the collection of $O(5 \times 10^{12})$ positrons on target. The nominal beam energy was $E_{beam} = 490$ MeV and the multiplicity was kept at the level of 100 positrons per 1 ns, leading to about 25000 positrons per bunch. A secondary positron beam produced by the closer to the experimental setup BTF target was used, which led to an increased beam-induced background. In the autumn, 2020 during the three months of data taking, the RUN-II, an additional sample with similar to RUN-I statistics was collected. However, the internal DAΦNE Linac positron converter was used. This limited the beam energy to $E_{beam} = 430$ MeV but decreased significantly the beam induced background.

3.1 Probing the dark sector

The main goal of PADME is to search for the existence of new light particles in positron on target annihilation. The process of interest is

$$e^+ + e^- \rightarrow \gamma + A'. \quad (3)$$

By reconstructing the 4-momentum of the recoil photon through measuring its energy and impact position in an electromagnetic calorimeter, the missing mass can be computed as

$$M_{miss}^2 = (\vec{P}_{e^+} + \vec{P}_{e^-} - \vec{P}_{\gamma})^2, \quad (4)$$

where \vec{P}_{e^+} and $\vec{P}_{e^-} = (m_e, \vec{0})$ are the beam positron and the target electron 4-momenta. The experimental signature is a peak appearing over a smooth background in the missing mass spectrum - a technique called bump-hunting.

The chosen technique is sensitive to invisible decays of the dark photon, namely $A' \rightarrow \chi\chi$, where χ could be the dark matter constituents. The reach in mass is limited by the positron beam energy, $m_{A'} < 23.7$ MeV, while the sensitivity on the dark photon relative interaction strength is determined by the statistics.

3.2 Inclusive measurement of two photon annihilation cross section

The design of PADME allows for exclusive reconstruction of multiphoton and multielectron final states. This extends the physics program of PADME allowing for precise studies of various electromagnetic processes in the O(100) MeV range. This interval, being the most difficult to measure experimentally, still lacks many measurements with sub-5% uncertainty. This includes Bremsstrahlung emission differential cross section, the multiphoton annihilation cross section, Bhabha scattering, pairs creation.

Using 10% of the data collected in RUN-II PADME measured the inclusive cross section $\sigma(e^+e^- \rightarrow \gamma\gamma(\gamma))$ for positron-in-flight annihilation for positron energy $E_{beam} = 430$ MeV. Two analysis strategies for $e^+e^- \rightarrow \gamma\gamma(\gamma)$ annihilation yield measurement were combined. The tag-and-probe identification of genuine two cluster events was based on searching for a probe photon with a given energy at a given azimuthal angle upon a successful identification of a tagged photon from an annihilation event. This approach also lead to a determination of the photon reconstruction efficiency. In the single photon selection a consistent with zero missing mass squared was required.

The final result

$$\sigma(e^+e^- \rightarrow \gamma\gamma(\gamma)) = (1.977 \pm 0.018_{stat} \pm 0.119_{syst}) \text{ mb} \quad (5)$$

is with a precision of $\sim 5\%$ [20] and is consistent with the Standard Model predictions, as seen in Fig. 2, where a comparison with previous measurements is also shown. The PADME result is the only and the most precise measurement with two photons tagging, for E_{beam} below 1 GeV.

4. Prospects

4.1 Probing X17 particle

In the autumn 2022 PADME experiment used a modified experimental setup to probe the existence of the X17 particle, as suggested by the observation of anomalous structure in ^8Be , ^4He ,

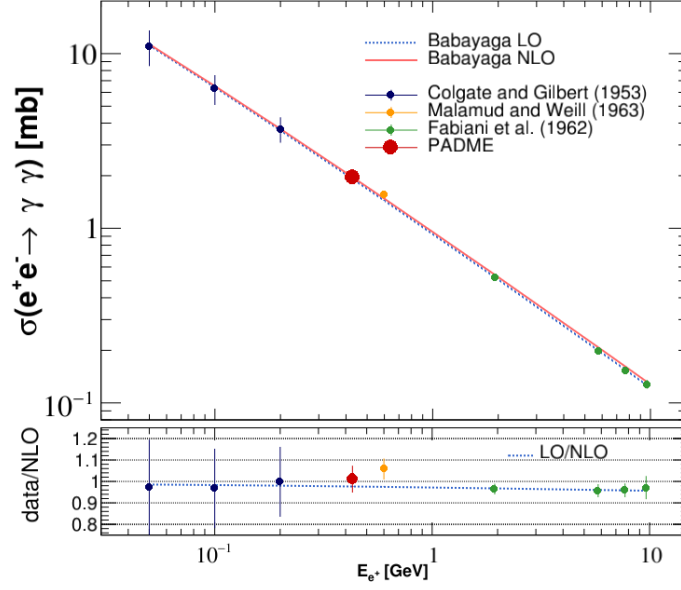


Figure 2: Measurement of the $\sigma(e^+e^- \rightarrow \gamma\gamma(\gamma))$ by PADME at $E_{beam} = 430$ MeV compared with previous measurements. The theory predictions at leading order and next-to-leading order are shown with lines. The ratio between data and theory for the different beam energy is also shown [20].

and ^{12}C deexcitations through internal pair creation. A resonance X17 production technique was adopted, where the beam energy is tuned to a center of mass value, matching the mass of X17. In the final state, the X17 decays into an electron-positron pair. The experimental signature is the observation of a change of the number of the detected e^+e^- pairs within a narrow beam energy interval, consistent with m_{X17} .

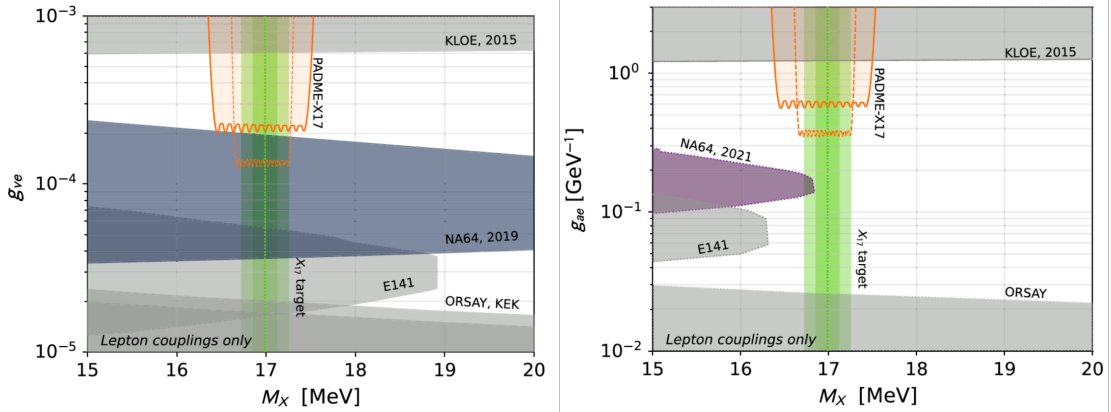


Figure 3: PADME expected sensitivity to a vector (left) and pseudo-scalar (right) boson [21].

The magnetic field of setup was set to 0 T and the detection of the final state particles was performed by the ECal. The charged particles and the $X17 \rightarrow e^+e^-$ signal identification was based on a newly constructed wall of plastic scintillators, a hodoscope, placed in front of the ECal. Considering the two viable options for X17, vector and pseudoscalar, the expected 90% confidence

level sensitivity of PADME RUN-III to the vector coupling (g_{ve}) and pseudo-scalar coupling (g_{ae}) is shown with orange line in Fig. 3.

4.2 Application of machine learning techniques

In the PADME experiment the high particle multiplicity (about $100 e^+$ per ns) results in multiple pulses in the individual detector elements of the experimental setup. The long decay time of the BGO, about 300 ns, makes the double pulse separation necessary, but a difficult task. A machine learning method based on convolutional neural networks was developed [22] aiming both at the identification and at the reconstruction of the properties of overlapping pulses in the ECal channels.

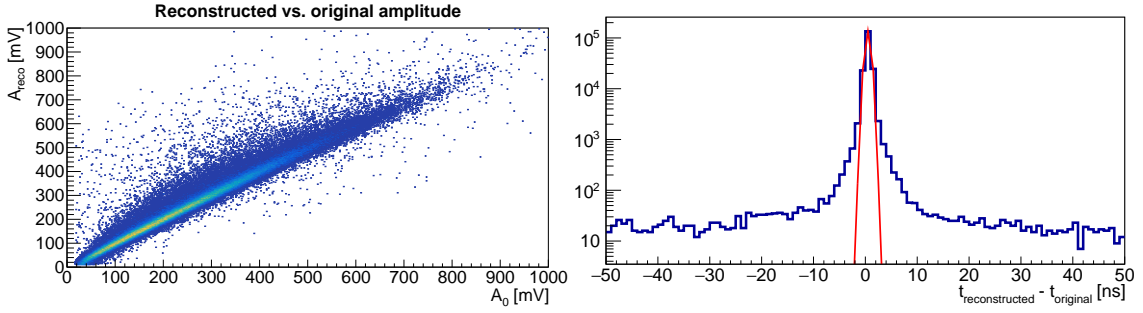


Figure 4: Reconstructed versus true amplitude of the pulses in an ECal channel (left) and difference between the reconstructed and the true time of the pulse (right) [22].

The topology of the neural network mimics an autoencoder but the desired output are the deconvoluted moments of particle energy deposits in the detecting elements. The initial results are promising as seen in Fig. 4 for the amplitude reconstruction (left) and the time reconstruction (right) with achievable time resolution of ~ 500 ps.

5. Conclusions

The PADME experiment at LNF-INFN probes the existence of new light particles with non-vanishing couplings to the Standard Model electrons. During three periods of running sufficient data was collected to achieve sensitivity down to an order of 10^{-6} in the relative interaction strength for the dark photon case, g_{ve} down to an order of 10^{-4} for vector X17, and $g_{ae} \sim 5 \times 10^{-1} \text{ GeV}^{-1}$ for pseudoscalar X17. In addition, several electromagnetic processes, like multiphoton annihilation, Bremsstrahlung emission, and Bhabha scattering are studied in details.

Acknowledgements

The authors acknowledge major support from Istituto Nazionale di Fisica Nucleare, Italy. Partial support has also been granted by: BG-NSF KP-06-DO02/4 from 15.12.2020 as part of MUCCA, CHIST-ERA-19-XAI-009; TA-LNF as part of STRONG-2020 EU Grant Agreement 824093; and BNSF through COST action CA21106 - COSMIC WISPerS in the Dark Universe.

References

- [1] B. Abi *et al.*, Phys. Rev. Lett. **126**, 141801, 2021.
- [2] A. J. Krasznahorkay, *et al.* Phys. Rev. Lett. **116** (2016) no.4, 042501.
- [3] A. J. Krasznahorkay, *et al.* [arXiv:2209.10795 [nucl-ex]].
- [4] A. J. Krasznahorkay, *et al.* Phys. Rev. C **104** (2021) no.4, 044003.
- [5] B. Holdom, Phys. Lett. B **166**, 196 (1986).
- [6] J. Alexander *et al.*, arXiv:1608.08632 [hep-ph] (2016).
- [7] M. Raggi and V. Kozhuharov, Riv. Nuovo Cim. **38**, no. 10, 449 (2015).
- [8] V. Kozhuharov and M. Naydenov, Nucl. Phys. B **986** (2023), 116044.
- [9] M. Raggi and V. Kozhuharov, Adv. High Energy Phys., **2014**, 959802, 2014.
- [10] M. Raggi, V. Kozhuharov and P. Valente, EPJ Web Conf. **96** (2015), 01025.
- [11] P. Valente, *et al.*, [arXiv:1603.05651 [physics.acc-ph]] (2016).
- [12] P. Valente, *et al.*, J. Phys. Conf. Ser. **874** (2017) no.1, 012017.
- [13] P. Albicocco, *et al.*, JINST **15** (2020) no.10, T10003.
- [14] I. Oceano [PADME], JINST **15** (2020) no.04, C04045.
- [15] A. Frankenthal, *et al.* Nucl. Instrum. Meth. A **919** (2019), 89-97.
- [16] G. Georgiev *et al.* IEEE Trans. Nucl. Science 65 (2018) 2029.
- [17] F. Oliva [PADME], JINST **15** (2020) no.06, C06017.
- [18] P. Albicocco, *et al.* [PADME], JINST **17** (2022) no.08, P08032.
- [19] F. Bossi *et al.* [PADME], JHEP **09** (2022), 233.
- [20] F. Bossi *et al.* [PADME], Phys. Rev. D **107** (2023) no.1, 012008.
- [21] Luc Darmé *et al.*, Phys. Rev. D **106** (2022) 11, 115036.
- [22] K. Dimitrova [PADME], Instruments **6** (2022) no.4, 46